Spider: dtiQA v7.1.1 (Multi)
Creation Date: June 1, 2020

Authors:
- Leon Cai (leon.y.cai@vanderbilt.edu)
- Qi Yang (qi.yang@vanderbilt.edu)

Run Date: 2020-06-15 22:25:18.026863

Project: LANDMAN_UPGRAD
Subject: 229415
Session: 229919

Parameters:
- BValue Threshold: 50
- Run Denoise: True
- Run Prenormalize: True
- Try Synb0-DisCo: True
- Extra Topup Args:
- Eddy Mask: True
- Extra Eddy Args:
- Run Postnormalize: False
- Run N4 Bias Field Correction: False
- Split Outputs: False
- Keep Intermediates: False

Preprocessing: Topup (RPE) + Eddy
Inputs (w/ PE direction and readout time):
- DTI_APA (j-, 0.05)
- WIP_HARDI_60_2_5iso (j+, 0.05)
- t1

Warnings (See "dtiQA_v7 Assumptions and User Guide" for more information):

- Each of the input diffusion volumes must have the same phase encoding axis, as input into this pipeline and as reflected above. Please see the PE Direction page of this PDF for more information.
- Eddy encountered an error while running and successfully reran when forced to run on non-shelled data, suggesting the input data was a non-shelled (i.e. DSI) image. Please note that eddy does not currently support DSI data and may produce spurious results. Please verify your data is shelled or that this behavior is expected.

Methods Summary:

The diffusion data were preprocessed and quality-checked with the following pipeline built around the MRTrix3 [1], FSL [2], and ANTs [3] software packages. First, any volumes with a corresponding b value less than 50 were treated as b0 volumes for the remainder of the pipeline. Then, the diffusion data were denoised with the provided dwidenoise function included with MRTrix3 [4][5]. The images were then intensity-normalized to the first image and concatenated for further processing. FSL's topup and eddy algorithms were used to correct for susceptibilty-induced and motion artifacts and eddy currents and to remove outlier slices [6][7][8][9]. Lastly, the preprocessed data were fitted with a tensor model using the dwi2tensor function included with MRTrix3 using an iterative reweighted least squares estimator [10]. The quality of this preprocessing pipeline was then assessed qualitatively for gross errors and quantitatively analyzed using a three-step approach. In the first step, the preprocessed data were analyzed in accordance with the method outlined by Lauzon et al. [11]. The brain parenchyma without CSF were masked in a restrictive manner by using an eroded brain mask generated on the average b0 image using the bet2 function included with FSL [12]. Then, the tensor fits of the masked data were backpropagated through the diffusion model to reconstruct the original diffusion signal. The goodness-of-fit for the tensor model was then assessed using a modified pixel chi-squared value per slice per volume. In the second step, the tensor fit was converted to a fractional anisotropy (FA) image [13][14]. The ICBM FA MNI atlas with 48 white matter tract labels provided with FSL were then non-rigidly registered to the subject's FA image with the ANTs software package [15][16][17][18]. The average FA for each tract was then quantified and assessed for physiologic congruence. Lastly, the gradient orientations were visualized and checked using the dwigradcheck script included with MRTrix [19].

References:

[1] Tournier, J. D. et al. (2019). MRtrix3: A fast, flexible and open software framework for medical image processing and visualisation. NeuroImage, 116137.
[2] Jenkinson, M. et al. (2012). Fsl. Neuroimage, 62(2), 782-790.
[3] Tustison, N. J. et al. (2014). Large-scale evaluation of ANTs and FreeSurfer cortical thickness measurements. Neuroimage, 99, 166-179.
[4] Veraart, J. et al. (2016). Denoising of diffusion MRI using random matrix theory. Neuroimage, 142, 394-406.
[5] Veraart, J. et al. (2016). Diffusion MRI noise mapping using random matrix theory. Magnetic resonance in medicine, 76(5), 1582-1593.
[6] Andersson, J. L. et al. (2003). How to correct susceptibility distortions in spin-echo echo-planar images: application to diffusion tensor imaging. Neuroimage, 20(2), 870-888.
[7] Smith, S. M. et al. (2004). Advances in functional and structural MR image analysis and implementation as FSL. Neuroimage, 23, S208-S219.
[8] Andersson, J. L. et al. (2016). An integrated approach to correction for off-resonance effects and subject movement in diffusion MR imaging. Neuroimage, 125, 1063-1078.
[9] Andersson, J. L. et al. (2016). Incorporating outlier detection and replacement into a non-parametric framework for movement and distortion correction of diffusion MR images. NeuroImage, 141, 556-572.
[10] Veraart, J. et al. (2013). Weighted linear least squares estimation of diffusion MRI parameters: strengths, limitations, and pitfalls. Neuroimage, 81, 335-346.
[11] Lauzon, C. B. et al. (2013). Simultaneous analysis and quality assurance for diffusion tensor imaging. PloS one, 8(4).
[12] Smith, S. M. (2002). Fast robust automated brain extraction. Human brain mapping, 17(3), 143-155.
[13] Basser, P. J. et al. (1994). MR diffusion tensor spectroscopy and imaging. Biophysical journal, 66(1), 259-267.
[14] Westin, C. F. (1997). Geometrical diffusion measures for MRI from tensor basis analysis. Proc. ISMRM'97.
[15] Mori, S. et al. (2005). MRI atlas of human white matter. Elsevier.
[16] Wakana, S. et al. (2007). Reproducibility of quantitative tractography methods applied to cerebral white matter. Neuroimage, 36(3), 630-644.
[17] Hua, K. et al. (2008). Tract probability maps in stereotaxic spaces: analyses of white matter anatomy and tract-specific quantification. Neuroimage, 39(1), 336-347.
[18] Avants, B. B. et al. (2008). Symmetric diffeomorphic image registration with cross-correlation: evaluating automated labeling of elderly and neurodegenerative brain. Medical image analysis, 12(1), 26-41.
[19] Jeurissen, B. et al. (2014). Automated correction of improperly rotated diffusion gradient orientations in diffusion weighted MRI. Medical image analysis, 18(7), 953-962.

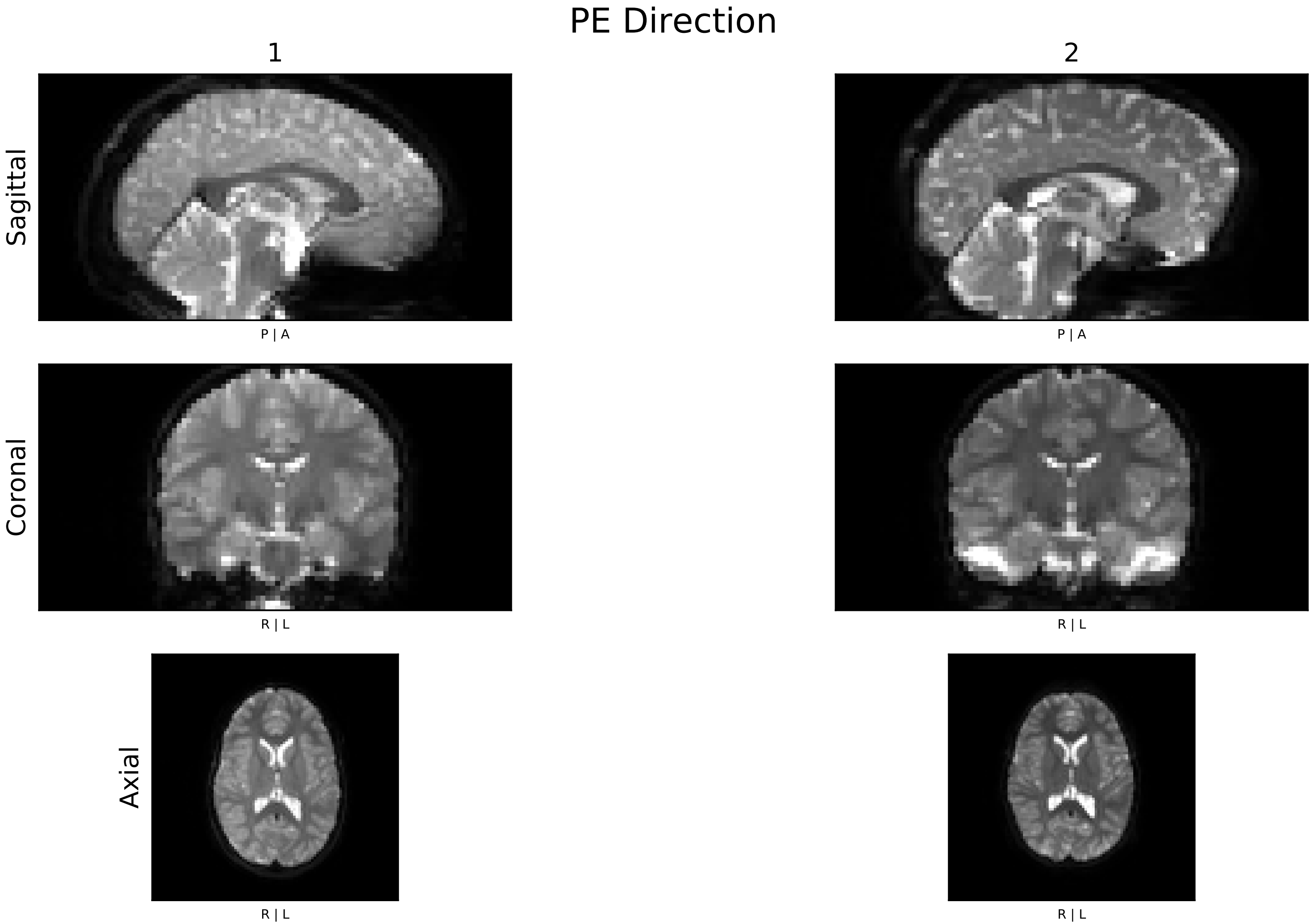

1) DTI_APA_checked (From A)
2) WIP_HARDI_60_2_5iso_checked (To A)

The supplied phase encoding direction for the input images was "j". Thus, the best interpreted anatomical axes for these images based on their affines are described to the left. Please ensure that these axes (direction agnostic) are interpreted to be the same and are visually distorted above for all images. It is an underlying assumption of this pipeline that all images be phase encoded on the same axis with varying direction as appropriate.

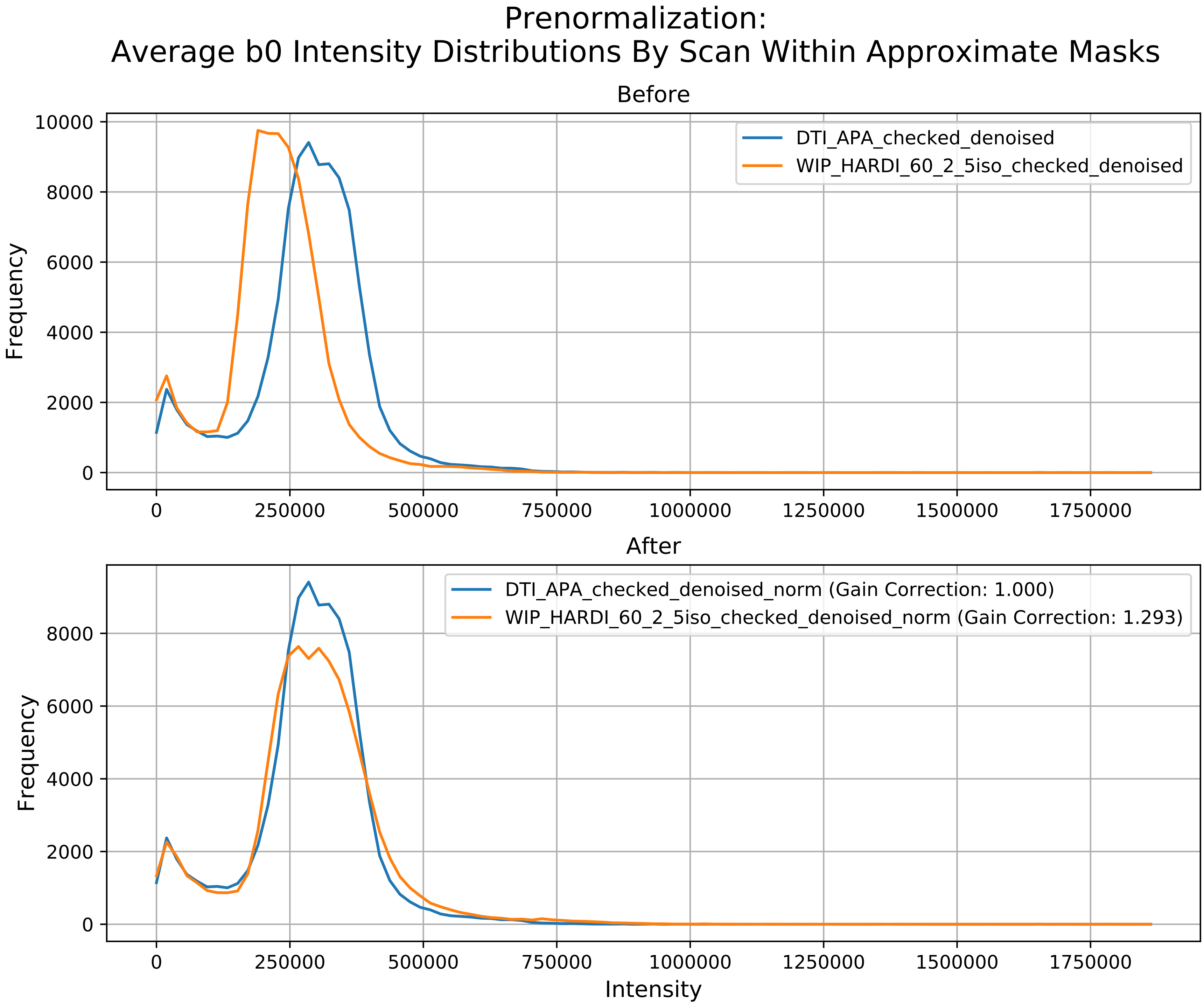
Prenormalization:
Average b0 Intensity Distributions By Scan Within Approximate Masks
Before
DTI_APA_checked_denoised
WIP_HARDI_60_2_5iso_checked_denoised
Frequency
10000
8000
6000
4000
2000
0
0
250000
500000
750000
1000000
1250000
1500000
1750000
After
DTI_APA_checked_denoised_norm (Gain Correction: 1.000)
WIP_HARDI_60_2_5iso_checked_denoised_norm (Gain Correction: 1.293)
Frequency
8000
6000
4000
2000
0
0
250000
500000
750000
1000000
1250000
1500000
1750000
Intensity

Preprocessing and Masks

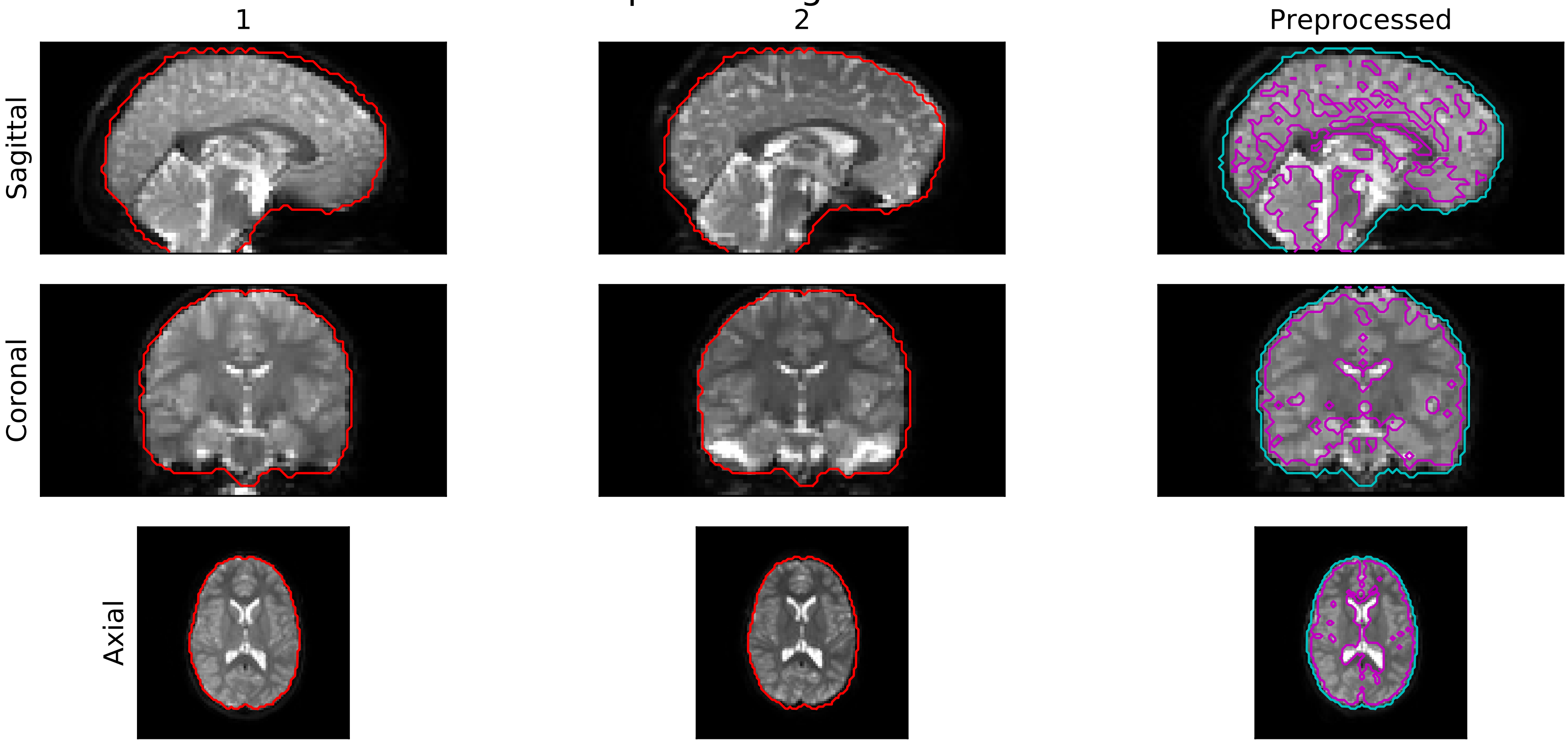

1) DTI_APA_checked
2) WIP_HARDI_60_2_5iso_checked

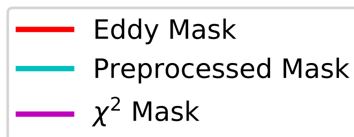

- Eddy Mask: If --eddy_mask is "on" (default), this is calculated on the averaged raw b0s if topup is not run and on the averaged topped-up b0s if it is. If --eddy_mask is "off", this mask is not applied and eddy is performed on the entire volume. This mask need only be approximate and is used for motion and eddy-current correction.
- Preprocessed Mask: This is calculated on the preprocessed averaged b0s. It is used for tensor visualization and other analyses (i.e. SNR and CNR calculations, gradient table checks, etc.) and is the basis for the chi-squared mask.
- Chi-Squared Mask: This is calculated from the preprocessed mask by subtracting the CSF and eroding the result. It is used to determine the voxels in which to perform the chi-squared analysis.

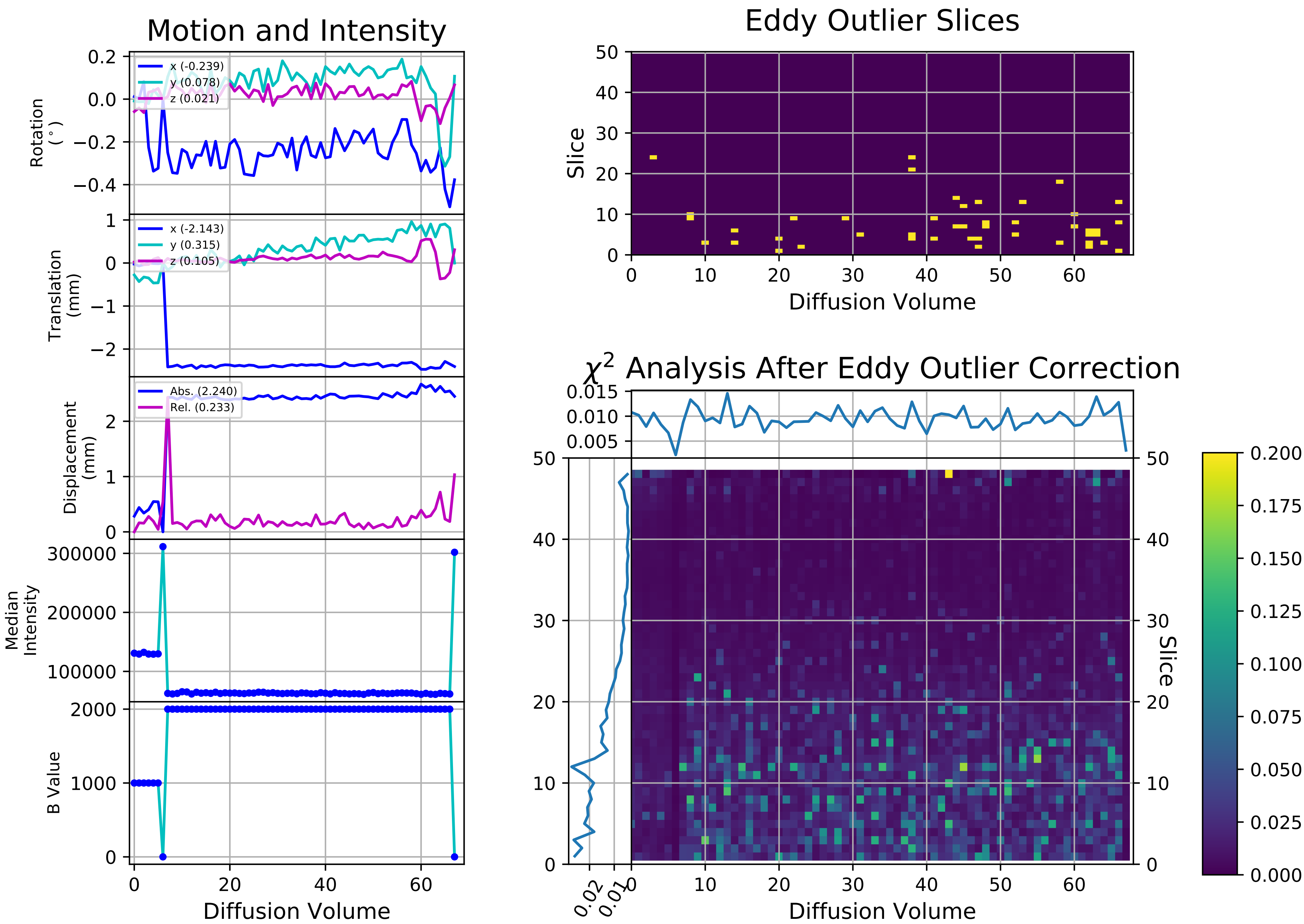

Motion and Intensity
Rotation (°)
x (-0.239)
y (0.078)
z (0.021)
Translation (mm)
x (-2.143)
y (0.315)
z (0.105)
Displacement (mm)
Abs. (2.240)
Rel. (0.233)
Median Intensity
B Value
Diffusion Volume
Eddy Outlier Slices
Slice
Diffusion Volume
χ^2 Analysis After Eddy Outlier Correction
Slice
Diffusion Volume

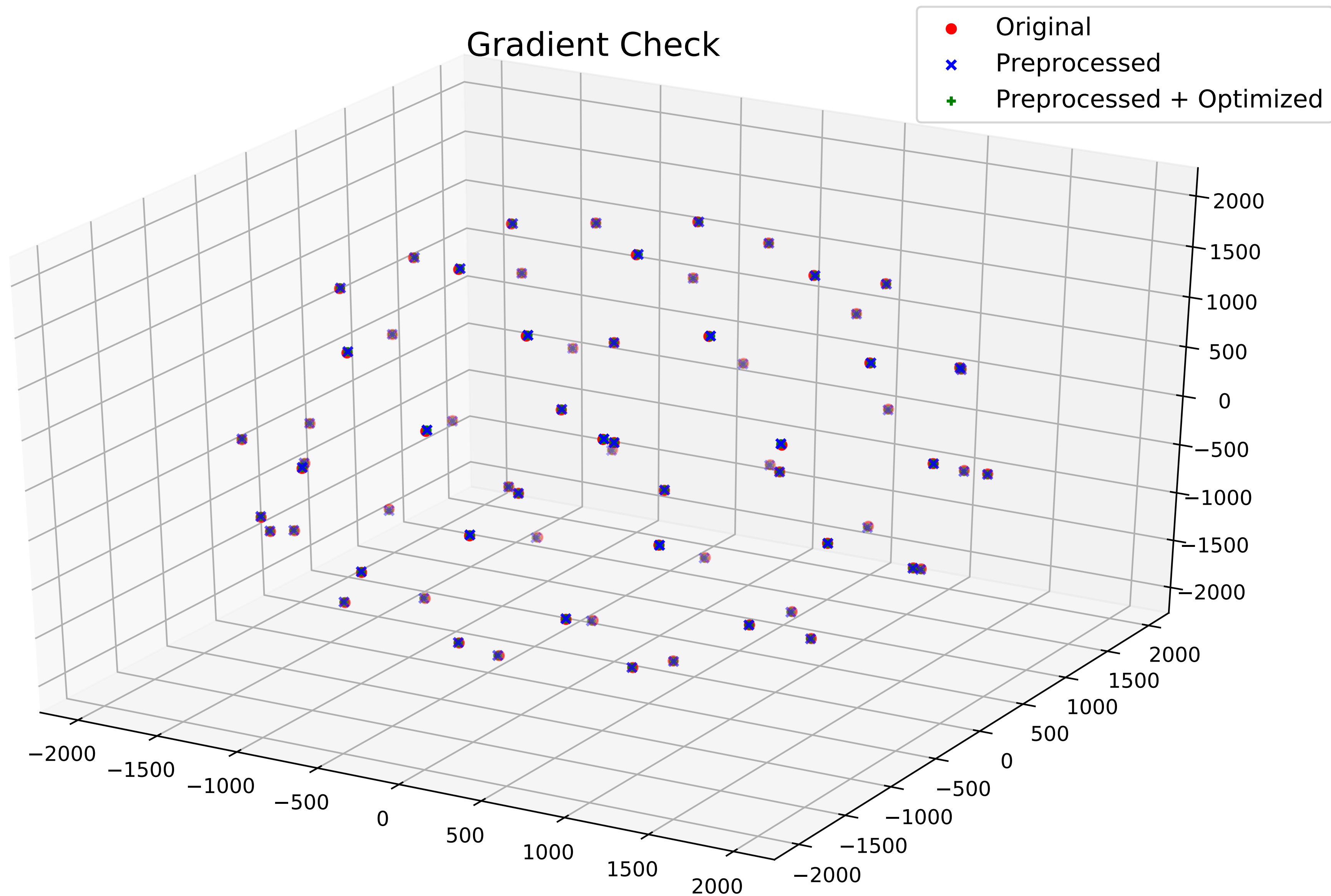

- Original: Raw gradients (b-vectors scaled by b-value) given as input.
- Preprocessed: Gradients output and rotated by eddy. Often slightly different than the original gradients.
- Preprocessed + Optimized: Preprocessed gradients that have been sign and order permuted to produce the optimal tract length as determined by dwigradcheck in MRTrix3. Ideally identical to the preprocessed gradients. If not, this suggests an incorrect sign or axis permutation in the b-vectors. Glyph visualization on the Tensor page of this PDF can help support this.

Preprocessed b = 0.0, 2 scan average, SNR = 19.612

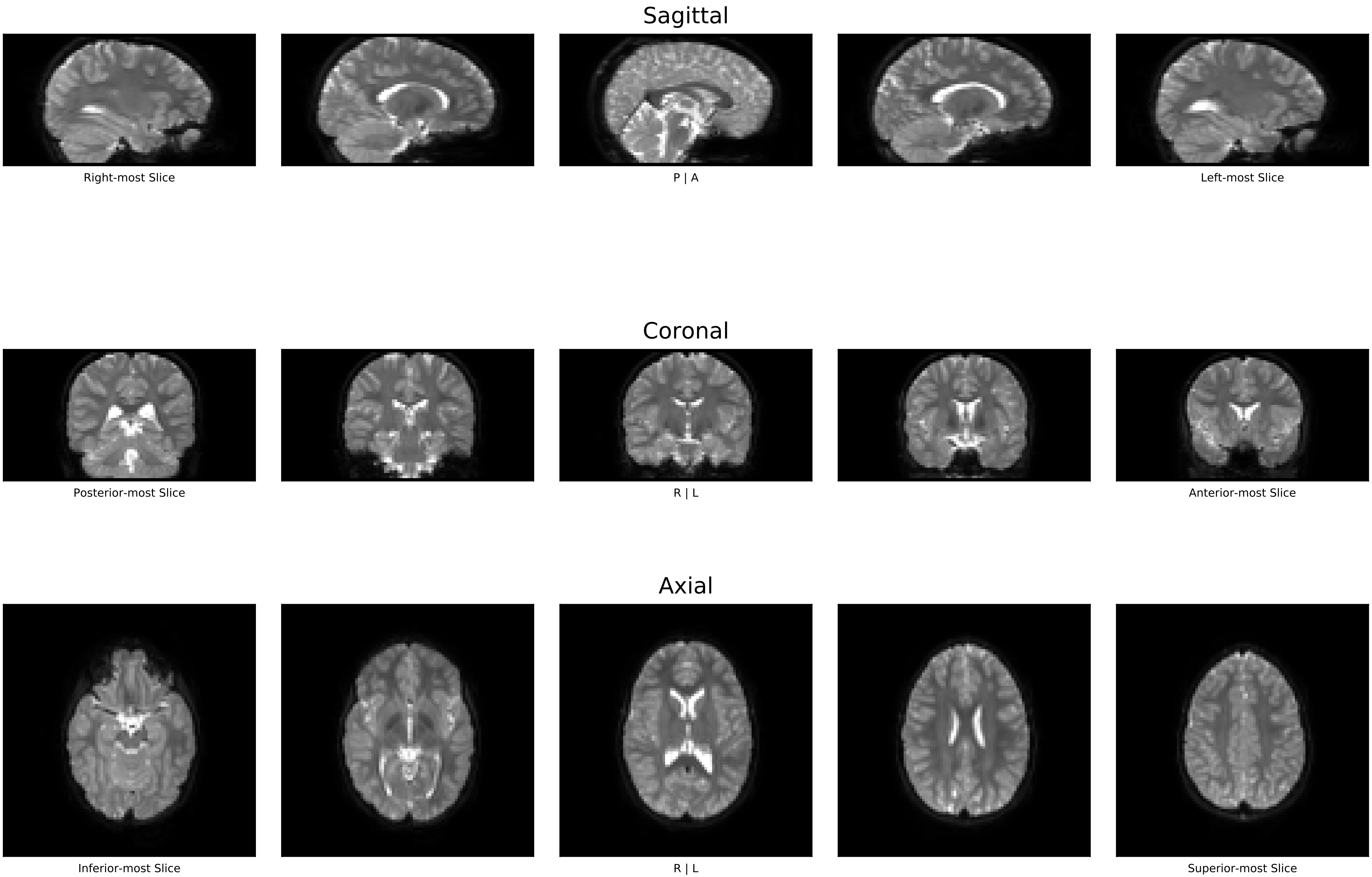

Preprocessed b = 1000.0, 6 scan average, CNR = 2.290

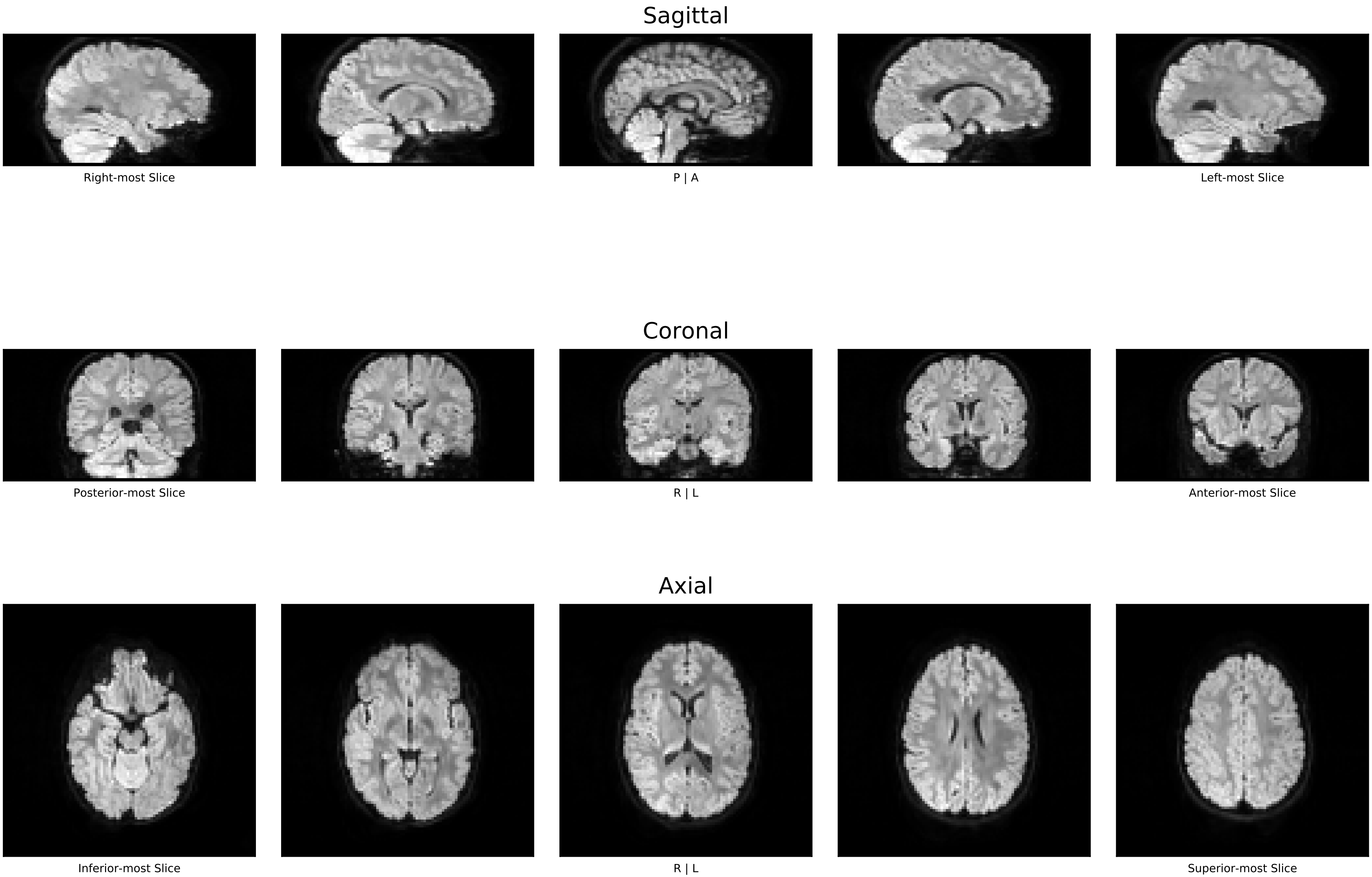

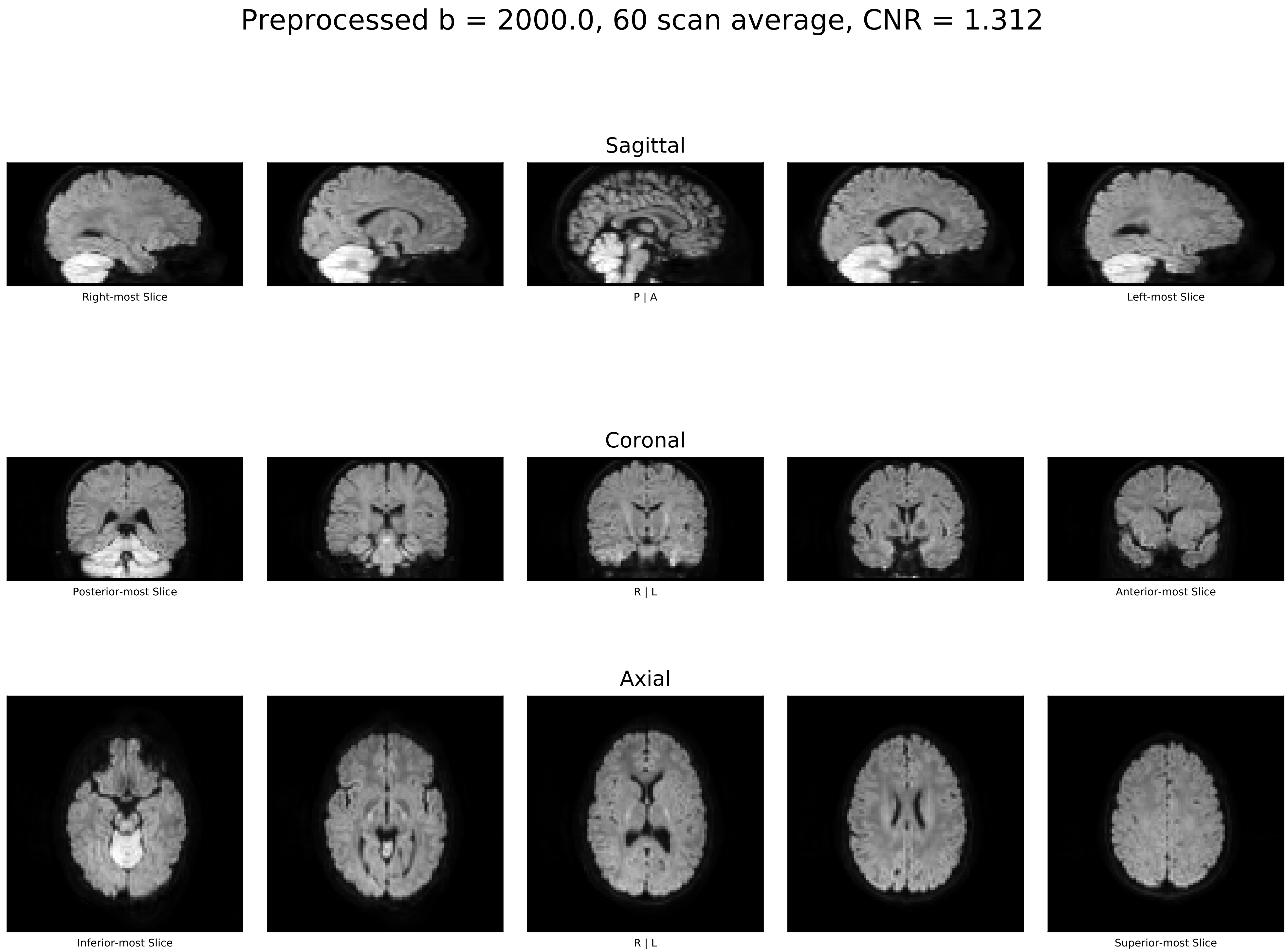
Preprocessed b = 2000.0, 60 scan average, CNR = 1.312
Sagittal
Right-most Slice
P | A
Left-most Slice
Coronal
Posterior-most Slice
R | L
Anterior-most Slice
Axial
Inferior-most Slice
R | L
Superior-most Slice

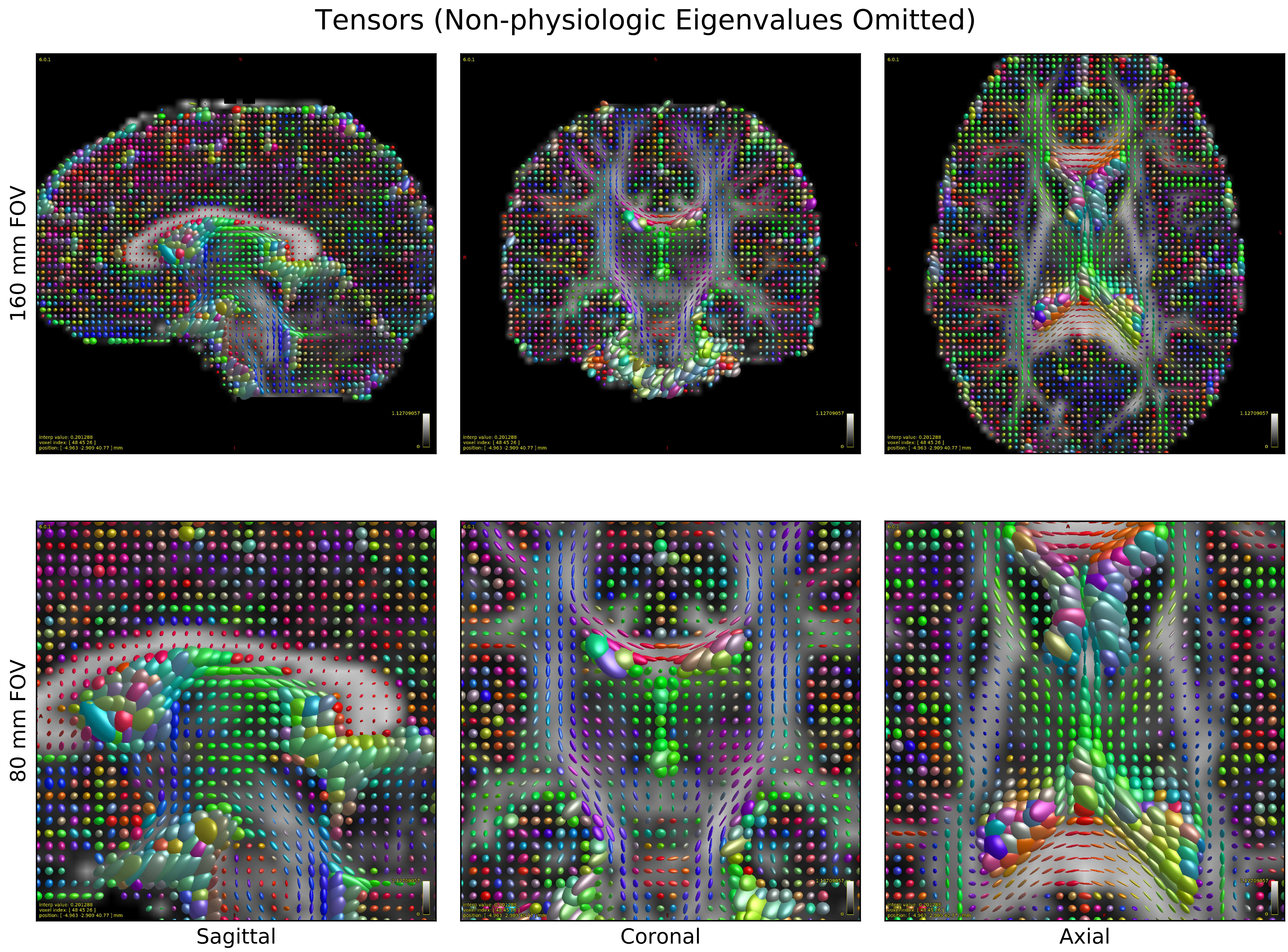
Tensors (Non-physiologic Eigenvalues Omitted)
160 mm FOV
80 mm FOV
Sagittal
Coronal
Axial

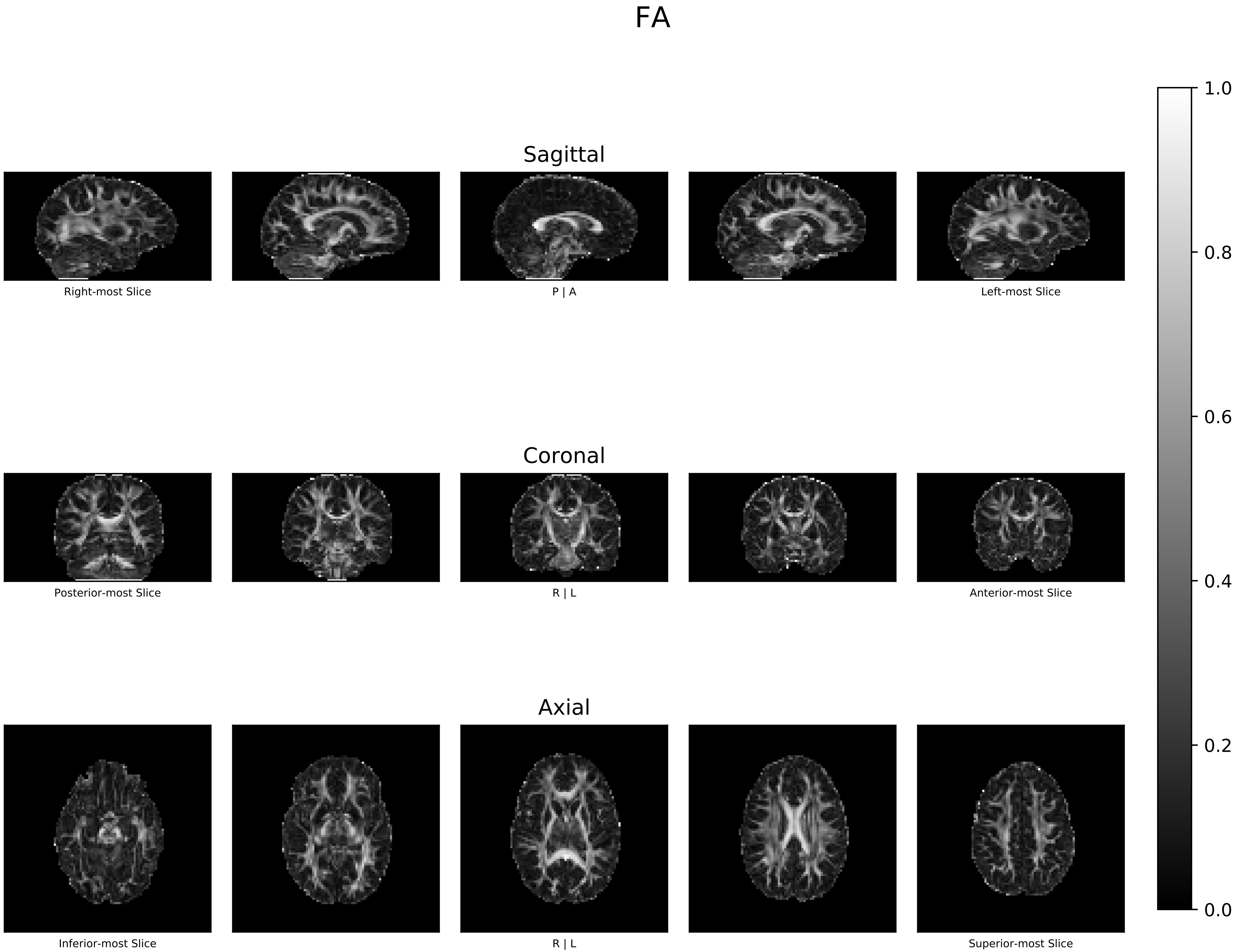
FA
Sagittal
Right-most Slice
P | A
Left-most Slice
Coronal
Posterior-most Slice
R | L
Anterior-most Slice
Axial
Inferior-most Slice
R | L
Superior-most Slice
1.0
0.8
0.6
0.4
0.2
0.0

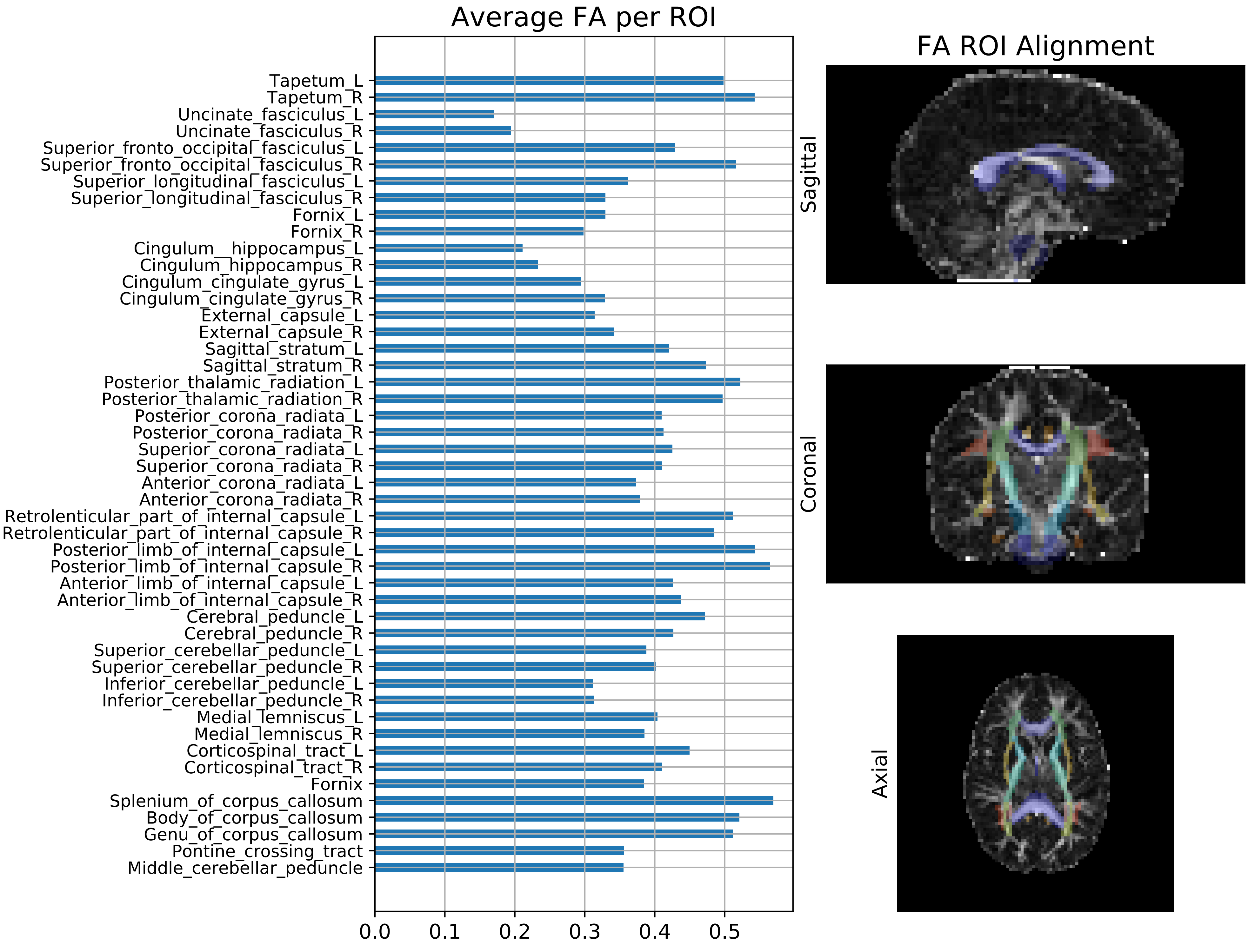
Average FA per ROI
Tapetum_L
Tapetum_R
Uncinate_fasciculus_L
Uncinate_fasciculus_R
Superior_fronto_occipital_fasciculus_L
Superior_fronto_occipital_fasciculus_R
Superior_longitudinal_fasciculus_L
Superior_longitudinal_fasciculus_R
Fornix_L
Fornix_R
Cingulum__hippocampus_L
Cingulum_hippocampus_R
Cingulum_cingulate_gyrus_L
Cingulum_cingulate_gyrus_R
External_capsule_L
External_capsule_R
Sagittal_stratum_L
Sagittal_stratum_R
Posterior_thalamic_radiation_L
Posterior_thalamic_radiation_R
Posterior_corona_radiata_L
Posterior_corona_radiata_R
Superior_corona_radiata_L
Superior_corona_radiata_R
Anterior_corona_radiata_L
Anterior_corona_radiata_R
Retrolenticular_part_of_internal_capsule_L
Retrolenticular_part_of_internal_capsule_R
Posterior_limb_of_internal_capsule_L
Posterior_limb_of_internal_capsule_R
Anterior_limb_of_internal_capsule_L
Anterior_limb_of_internal_capsule_R
Cerebral_peduncle_L
Cerebral_peduncle_R
Superior_cerebellar_peduncle_L
Superior_cerebellar_peduncle_R
Inferior_cerebellar_peduncle_L
Inferior_cerebellar_peduncle_R
Medial_lemniscus_L
Medial_lemniscus_R
Corticospinal_tract_L
Corticospinal_tract_R
Fornix
Splenium_of_corpus_callosum
Body_of_corpus_callosum
Genu_of_corpus_callosum
Pontine_crossing_tract
Middle_cerebellar_peduncle
0.0
0.1
0.2
0.3
0.4
0.5
FA ROI Alignment
Sagittal
Coronal
Axial

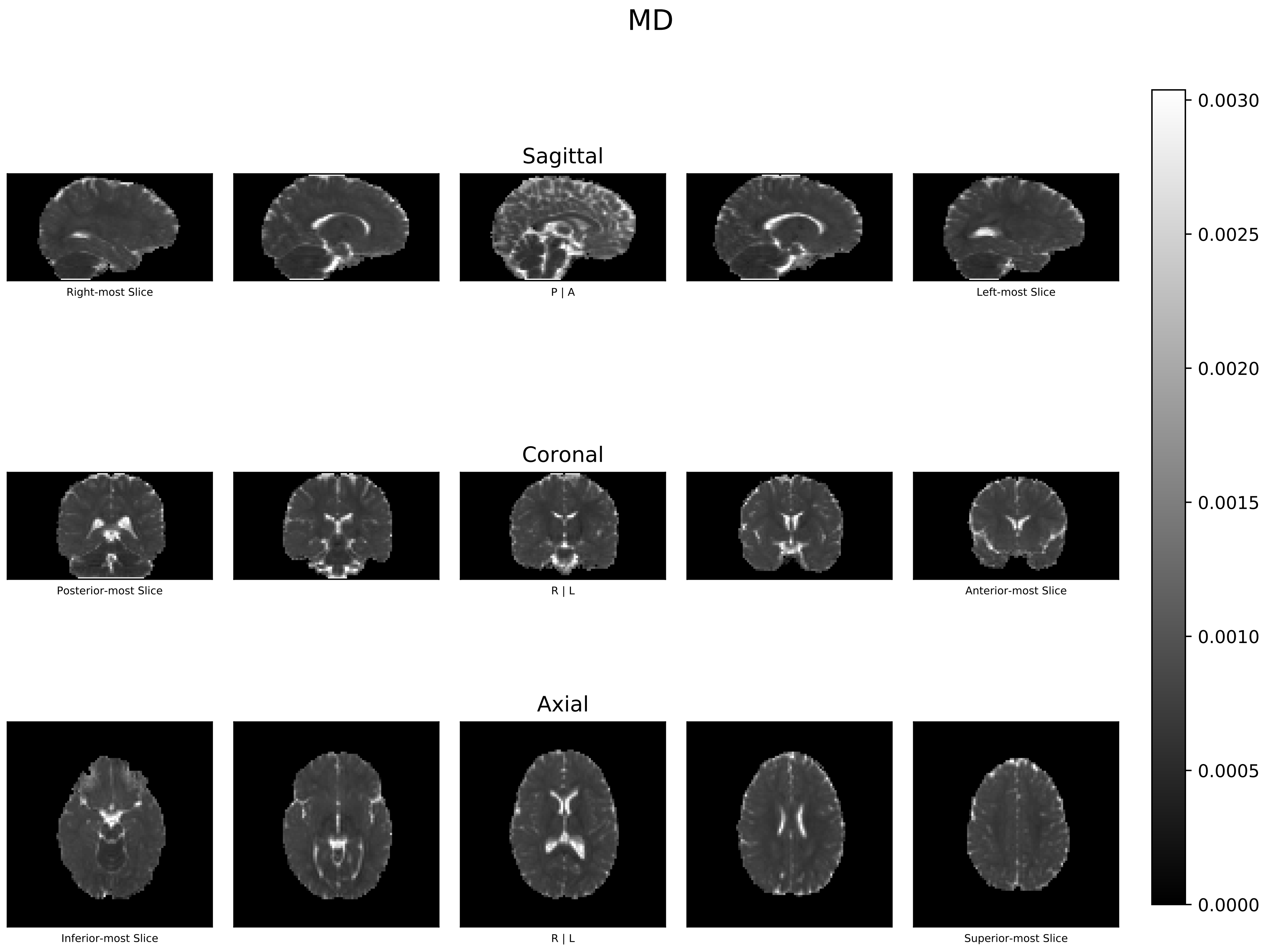
MD
Sagittal
Right-most Slice
P | A
Left-most Slice
Coronal
Posterior-most Slice
R | L
Anterior-most Slice
Axial
Inferior-most Slice
R | L
Superior-most Slice
0.0030
0.0025
0.0020
0.0015
0.0010
0.0005
0.0000